

In situ and *ex vivo* evaluation of a wireless magnetoelastic biliary stent monitoring system

Scott Ryan Green · Richard S. Kwon · Grace H. Elta · Yogesh B. Gianchandani

Published online: 24 February 2010
© Springer Science+Business Media, LLC 2010

Abstract This paper presents the *in situ* and *ex vivo* evaluation of a system that wirelessly monitors the accumulation of intimal tissue and sludge in a biliary stent. The sensing element, located within the stent, is a magnetoelastic resonator that is queried by a wireless radio frequency signal. The *in situ* testing uses a commercially-available self-expanding biliary stent enhanced with a 1 mm×25 mm magnetoelastic ribbon sensor (formed from Metglas™ 2605SA1). The stent has a conformal magnetic layer (consisting of strontium ferrite particles suspended in polydimethylsiloxane) that biases the sensor. The external interrogation module is able to acquire a signal from the sensor from a distance of at least 5 cm while the sensor is implanted in a porcine carcass and loaded with biological fluids. The *ex vivo* testing uses bile harvested from the porcine carcass. The response of a 1 mm×25 mm magnetoelastic ribbon sensor is first calibrated with fluids of known density and viscosity, and the calibrated sensor is used to estimate that the viscosity of the harvested bile is 2.7–3.7 cP. The test results presented in this paper illustrate

the fundamental usability of the system when the sensor is implanted, loaded by biological fluids, and interrogated in a surgical setup.

Keywords Implant · Resonant sensors · Biliary sludge · Mass sensors · Viscosity sensors

1 Introduction

Stents are tubular structures used to establish and maintain patency in a variety of blood vessels and ducts within the gastrointestinal tract that have become obstructed as a result of benign or malignant pathology. Though the act of implanting a stent often relieves acute symptoms caused by the obstruction, stents are also at risk for obstruction due to accumulation of luminal contents such as ingrowth of normal or malignant tissue.

An example of a stent application area—and the focus of this work—is the bile duct. For metal stents which are used to palliate malignant biliary obstructions, blockage can occur in an unpredictable timeframe of 2–12 months via two main processes that can occur separately or in tandem. The first process is proliferation of intima or tissue ingrowth (Kozarek 2000); the second process is formation of a bacterial matrix on and around the stent known as biliary “sludge” (Donelli et al. 2007; Sung 1995). The tissue and sludge accumulate and eventually lead to occlusion of the duct and a reappearance of symptoms related to blockage, including jaundice and pruritus, and puts the patient at risk for cholangitis (infection of the bile duct), which can be fatal.

The initial method to diagnose a biliary obstruction is the measurement of serum concentration of liver enzymes such as bilirubin and alkaline phosphatase, among others. Unfortunately, enzyme levels may not rise until after the

S. R. Green (✉) · Y. B. Gianchandani
Department of Mechanical Engineering, University of Michigan,
Ann Arbor, MI, USA
e-mail: greensr@umich.edu

Y. B. Gianchandani
e-mail: yogesh@umich.edu

R. S. Kwon · G. H. Elta
Department of Internal Medicine - Gastroenterology,
University of Michigan,
Ann Arbor, MI, USA

Y. B. Gianchandani
Department of Electrical Engineering and Computer Science,
University of Michigan,
Ann Arbor, MI, USA

blockage is significant, resulting in delayed intervention. Alternatively, endoscopic retrograde cholangiography can be performed to image the duct and diagnose a blockage, but this specialized endoscopic procedure is invasive and has a risk of complications and therefore is generally reserved only for therapeutic purposes. A direct, non-invasive method of diagnosis would enable timely intervention and eliminate unnecessary procedures.

The method outlined in Fig. 1 highlights an integrated system providing just such a direct, non-invasive measurement of sludge and tissue accumulation in a biliary stent. The implanted device utilizes a self-expanding metal stent (although tubular polymeric stents could also be used) coated with a permanent magnet layer that provides a uniform and consistent bias field to the integrated magnetoelastic sensor. The sensor is integrated along the inner sidewall of the stent to maintain an open flow channel and is queried remotely by a wireless radio frequency signal. External to the patient, circuitry drives coils to produce an alternating magnetic field. The magnetic field causes the magnetoelastic sensor to resonate with a response which changes as local viscosity increases and as sludge and tissue accumulate. The response of the sensor is correlated to the local sensor environment—for example, the resonant frequency and quality factor can be used to measure the accumulated mass and bile viscosity.

We have previously reported on the basic architecture of the system, as well as the system performance in controlled bench-top testing with synthetic waxes and polymers used to mimic the biological loading (Green and Gianchandani 2009).

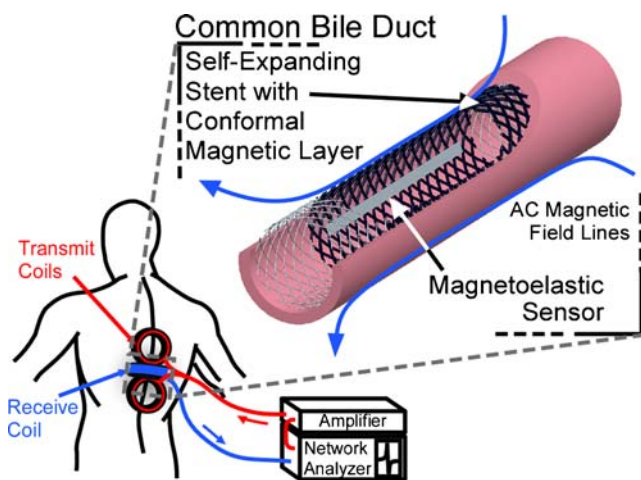


Fig. 1 Conceptual diagram of the magnetoelastic monitoring system used in the porcine carcass *in situ* experiment. A commercial self-expanding biliary stent (partially cut away in this figure to aid visualization of the sensor) is modified with a conformal magnetic layer that biases an attached magnetoelastic ribbon sensor. External circuitry drives the external interrogation coils to wirelessly measure the response of the implanted sensor. As sludge and tissue accumulate the frequency response of the sensor changes in a correlated manner

This paper describes the first results from *in situ* tests on a porcine carcass, performed in a surgical setting, as well as *ex vivo* tests using harvested bile. This work also explores the feasibility of integrating a magnetoelastic sensor into a commercial self-expanding stent. Survivability of the sensor and magnetic layer after assembly into the delivery system and subsequent deployment is addressed, along with issues related to the external interrogation module.

The design and fabrication of the sensor, magnetic layer, and interrogation module are presented in Section 2. Experimental methods and results are provided in Section 3. Section 4 describes additional steps that would be appropriate for future efforts, and describes the conclusions that can be drawn from this work.

2 Design and fabrication

Magnetoelastic sensor Magnetoelastic transduction is a term used to describe the coupling between the classical properties of stress and strain and the quantum phenomenon of magnetism (Engdahl 2000). Magnetoelastic behavior is most prominent in materials with strong coupling between the magnetic moment direction and the orientation of the elongated (anisotropically shaped) atom. Under an applied magnetic field, the coupled moments and atoms tend to rotate and align with the field, so that the magnetization and strain of the material is affected. From a macroscopic perspective, magnetoelastic coupling describes how the magnetization response to a magnetic field is related to the strain. For magnetoelastic materials used as resonant sensors, a simplified but useful understanding of the phenomenon would result from viewing the sensor as an oscillating dipole magnet, with the oscillations driven by the interrogative magnetic field. The oscillating magnetic flux developed in the sensor can then induce a voltage on a suitably located pick-up coil. Changes in resonance characteristics, such as resonant frequencies and quality factors, are used to determine mass loading and viscosity (Green and Gianchandani 2009).

For simplicity, $1\text{ mm} \times 25\text{ mm} \times 25\text{ }\mu\text{m}$ thick magnetoelastic ribbon-shaped sensors are chosen for this investigation. (More complex designs can be envisioned for enhanced functionality such as spatially localized sensing of the mass loads (Green and Gianchandani 2010)). The sensors are fabricated from Metglas™ 2605SA1 using the photochemical machining process (ASM 1989). To improve the signal amplitude and lower the required biasing field, the sensors are annealed for 1 h at 413°C in a 1.5 kOe transverse magnetic field. The sensor is bonded to the stent at the mid-length (vibrational node) of the sensor. For this work, the sensor is bonded to the coated stent using a small amount of polydimethylsiloxane (PDMS, Dow Sylgard

184), which is cured at 100°C for 1 h. A coated stent with an integrated sensor is shown in Fig. 2.

Biliary stent This work utilizes the smallest and shortest self-expanding metal stents that are typically used in human patients, in keeping with the expected small size of the common bile duct of the intended animal subject (Boston Scientific Wallstent™, 8 mm diameter × 60 mm length, Fig. 3). A stent, which is a braided Elgiloy™ (cobalt-chrome-nickel) mesh (Nelson 2001), is packaged within a delivery catheter assembly, which consists of an outer sheath over the compressed stent and introducer catheter. To deliver the stent, the introducer catheter is inserted into the bile duct over a guidewire. The outer sheath is retracted while the introducer catheter and guidewire are held stationary. As the sheath is retracted, the underlying stent elastically expands until it is fully deployed. For this work, the stent is mounted in the delivery assembly after coating with the conformal magnetic layer and bonding of the sensor.

Conformal magnetic layer The magnetic bias required by the sensor element is provided by a distributed conformal magnetic layer that is coated on the stent. This layer consists of strontium ferrite (SrFe) particles (~1 μm average diameter, Hoosier Magnetics) suspended in polydimethylsiloxane (PDMS, Sylgard 184, Dow Corning). The flexibility of the elastomeric PDMS base, along with its ability to closely conform to the struts of the stent, is intended to

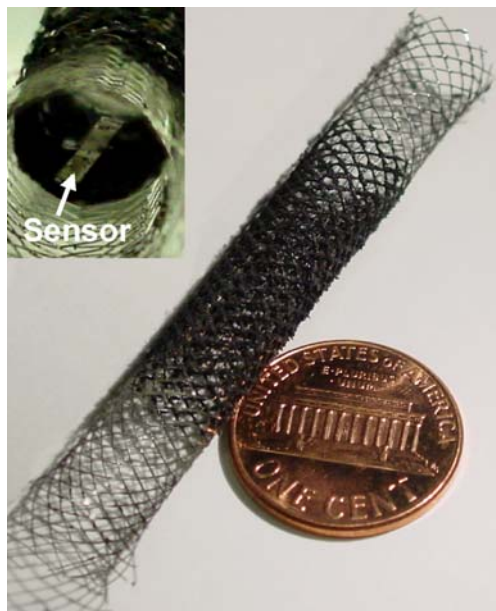


Fig. 2 8 mm×60 mm biliary stent after integration of sensor and conformal magnetic layer. The inset shows a view of the stent lumen and attached sensor. The ends of the stent are masked during the conformal magnetic layer coating procedure

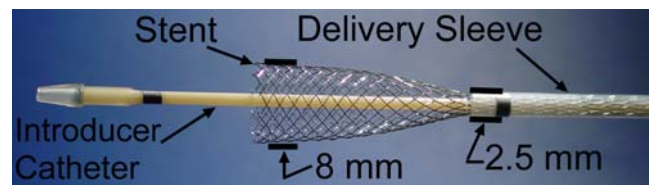


Fig. 3 Partially deployed 8 mm×60 mm self-expanding biliary stent (Wallstent™, Boston Scientific). Subsequent to integration of the conformal magnetic layer and magnetoelastic sensor, the stent is placed back in the delivery system after modification to the delivery sleeve diameter

minimize impact on the mechanics of the self-expanding stent. PDMS is accepted as a biocompatible material (Colas and Curtis 2004) and SrFe particles are chemically inert as a result of their ceramic nature, so this composite is expected to be appropriate for a chronically implanted application.

In this work, a 3:1 SrFe-PDMS ratio is used, applied in a 225 μm thick layer. First, the SrFe-PDMS mixture is spread in a thin layer of an approximately uniform thickness on a planar substrate. The ends of the stent are masked using thin adhesive tape, and then the stent is rolled along the SrFe-PDMS layer. As the stent struts contact the SrFe-PDMS, the magnetic composite adheres to the struts in a thin layer. The masking tape is removed and the magnetic composite is then cured at 150°C for 45 min. Additional coats can be used to build up the thickness of the layer (and increase the resulting magnetic field). For example, two coats covering the middle 30 mm of the length of the stent and applied in this manner result in a 1.1 Oe field from a layer approximately 150 μm thick, while the application of three coats results in a 1.65 Oe field from a layer approximately 225 μm thick as used in the final device. Application of multiple thin coats leads to better control of uniformity compared to the application of one thick coat. Note that the mechanical properties of the thick, high SrFe-content layer are adequate but less than ideal, especially in terms of repositioning the stent into the delivery system. The magnetic layer mechanical properties may be improved in the future by using higher strength magnetic particles.

Delivery system assembly After coating the stent and integrating the sensor, the assembly must be placed into the delivery system. In this initial work, a 4 mm diameter delivery catheter replaces the original 2 mm diameter delivery catheter, in order to accommodate the PDMS coating. The 4 mm diameter delivery catheter is compatible with standard endoscopic equipment. Trial assembly and deployment of the coated stent and integrated sensor shows that the sensor signal remains consistent before and after assembly and deployment. Also, the stent continues to reach its fully expanded diameter despite the presence of the conformal magnetic layer.

Interrogation module The extracorporeal sensor interface used in this work uses orthogonally-mounted transmit and receive coils, allowing both coils to couple with the sensor while minimizing coupling with each other. The transmit coils are located on both sides of the receive coil. The receive coil is elongated in one direction and flattened in the perpendicular direction (see Fig. 4). This arrangement allows most of the cross-sectional area of the receive coil to be closer to the sensor while existing in a null point of the transmitted signal. The number of turns per meter in the dual-layered transmit coils are chosen to improve the signal-to-noise ratio for this setup. In comparison to a previously used coil configuration, this configuration boosts the signal-to-noise ratio of the system by a factor of 2 (Green and Gianchandani 2009).

3 Experimental

3.1 Characterization and calibration

Conformal magnetic layer The remanent magnetic moment and coercivity is measured on SrFe:PDMS samples with 1:1 and 2:1 by-weight ratios using a vibrating sample magnetometer (courtesy of Princeton Measurements Corporation). The samples are 4 mm discs, each 100 μm thick. Two samples of each ratio are measured as a preliminary quantification of process repeatability. Typical hysteresis curves measured using the vibrating sample magnetometer are shown in Fig. 5. Note that the remanent magnetic moment is proportional to the by-weight ratio of SrFe:PDMS in this range of ratios. Additionally, the coercive force is consistent regardless of by-weight ratio. These



Fig. 4 Extracorporeal configuration used in the *in situ* testing as fabricated, with important dimensions. Coaxial cable connections to the pickup coil and transmit coils are on the back of the mount

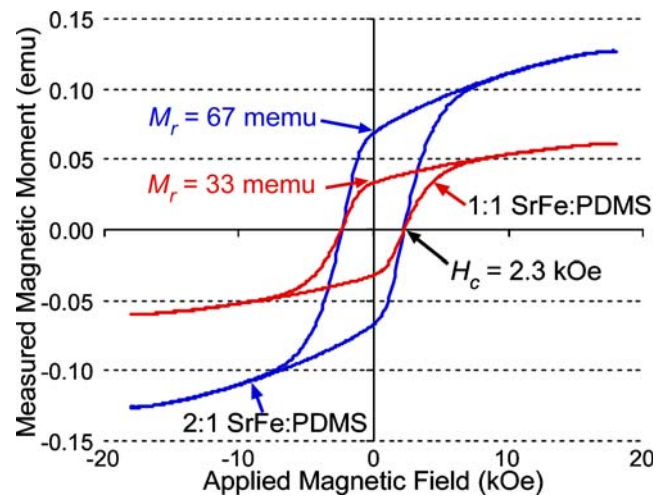


Fig. 5 M-H hysteresis curves for 4 mm diameter, 100 μm thick discs of SrFe-PDMS in different ratios. Note that the remanent magnetic moment (M_r) is proportional to the particle-to-polymer ratio

findings are consistent with previous work with polymer-particle composite magnets (Lagorce and Allen 1997). The resulting bias field is proportional to the thickness of the coating, which is generally controlled by the number of coats applied. Also, the resulting bias field is stronger for a stent with a smaller diameter assuming all other factors are equal (coating thickness, stent pattern, particle-to-polymer ratio, etc.). For example, a 6 mm diameter stent with a 100 μm thick coating of 1:1 SrFe-PDMS provides a bias field strength of approximately 0.5 Oe.

Transmit and receive coils The spatial performance of the extracorporeal configuration used in this work is experimentally characterized in Fig. 6. A 2 mm \times 37.5 mm \times 25 μm sensor is placed (in air) at various locations within the range of the interrogation coils. The measured signal amplitude is recorded at each location, and normalized to the signal amplitude measured when the sensor is centered with the coils and 7.5 cm from the face of the coils. In Fig. 6(a), the sensor is aligned parallel with the X axis (cranial-caudal). In the Z direction (posterior-anterior), the signal scales with $1/z^3$. In the X (cranial-caudal) and Y (medial-lateral) directions, the signal is symmetrically distributed. Spreading the transmit coils out results in a small improvement in the available signal as the sensor is offset in the X direction. In Fig. 6(b), the sensor has been rotated in the X-Z plane by 45° as shown in the inset schematic. Note that this rotation mimics the posterior-anterior angulation of a typical bile duct. This rotation results in a larger signal being available when the sensor is offset in the negative X direction such that the sensor is aligned with the field lines coming out of the transmit coils. However, an offset in the positive X direction results in a much smaller available signal because the field lines

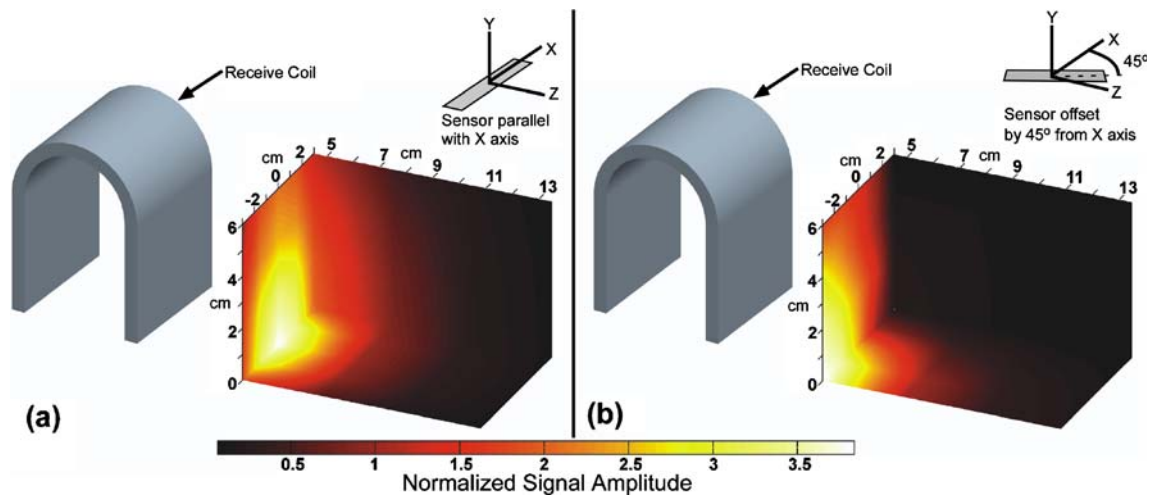


Fig. 6 Experimental spatial characterization of extracorporeal configuration used in the *in situ* testing. The signal amplitude is normalized to that available from the sensor at the coordinates (0, 0, 7.5 cm) and

parallel with the X axis. **(a)** Sensor aligned parallel with faces of coils. **(b)** Sensor rotated 45° in the X-Z plane. The spatial characteristics of both sensor alignments are symmetrical about the X-Z plane

emanating from the transmit coils are now mostly transverse to the sensor. For a sensor that is parallel with the X axis, at least 80% of the signal available at (0, 0, 7.5 cm) is available with an X offset of ± 3 cm, or with a Y offset of ± 5 cm. The measured resonant frequency varies only by approximately $\pm 0.3\%$ over the entire measured volume.

For the *ex vivo* tests described in Section 3.3, a coaxial coil configuration is used. Important parameters comparing the two configurations are listed in Table 1. The interrogation coils in both experiments are driven and measured by a HP4395A network analyzer, with the driven signal amplified by a commercial power amplifier (Krohn-Hite).

Although the design of the extracorporeal configurations is intended to place the receive coils at a null point of the transmitted signal, there is still a certain amount of coupling between the transmit and receive coils that results in an induced voltage on the receive coil. The amplitude and phase of the induced voltage is frequency dependent, and in general the frequency dependence is large enough to obscure the frequency response of the sensor unless subtracted from the overall signal measured while the sensor is present. Hence, a baseline measurement is first taken in the absence of the sensor, permitting the sensor signal to be recorded differentially. This method of measurement compensates for inductive coupling to fixed objects in the measurement environment, including medical furniture like a surgical table or chair.

Sensor response to viscosity A 1 mm wide \times 25 mm long \times 25 μm thick ribbon sensor (Metglas™ 2605SA1), that has been photochemically machined and transverse field annealed (1 h at 413°C in a 1.5 kOe transverse magnetic field), is calibrated using fluids of known density and

viscosity (Dow Corning 200 fluid (2 cS, 5 cS, 10 cS, 20 cS), air, and DI water), with the phase dip half-power bandwidth (Δf) over the phase dip center frequency (f_0) being the relevant measurement. Recorded center frequencies range from 58.5 kHz (for 20 cS fluid) to 63.6 kHz (for air). As shown in Fig. 7, the response of the sensor is proportional to the square root of the viscosity-density product for fluids in this range.

3.2 *In situ* experiment

As part of a separate medical study being conducted at the University of Michigan, a 30 kg female domestic pig was

Table 1 Comparison of coil configurations used in this work

	Coaxial	Extracorporeal
Transmit Coil Diameter (cm)	15.7	13
Transmit Coil Turns/Length (1/m)	588	1120
Transmit Coil Length (cm)	8	5
Receive Coil Dimensions (cm)	10.3 (dia.)	5 wide \times 13 tall
Receive Coil Turns/Length (1/m)	614	620
Receive Coil Length (cm)	4.4	5
Longitudinal AC Magnetic Field Amplitude at Sensor @ 60 kHz (A/m) (7.5 cm from extracorporeal setup)	20.5	6.5
Current Amplitude in Transmit Coil @ 60 kHz (mA)	38	87
SNR for Unloaded 2 mm \times 37.5 mm 2826 MB Ribbon Sensor (7.5 cm from extracorporeal setup)	210	50

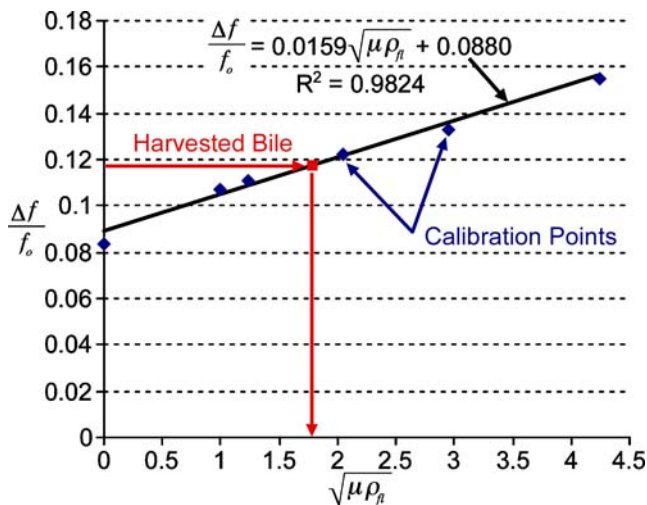


Fig. 7 The sensor response in harvested bile is compared to the response of the sensor in fluids of known properties. The response of the sensor indicates that the viscosity of the bile can be estimated as 2.75–3.68× that of water

ethanized and a necropsy was performed¹. For this study, the duodenum was opened and the biliary orifice was identified. Due to the small size of the bile duct (2 mm diameter) in comparison to the delivery system, a portion of the small intestine near the bile duct was clamped so that it formed a lumen of approximately 6 mm in diameter, which is more representative of the diameter of a human bile duct. The stent delivery system was then advanced into this simulated bile duct and the stent deployed within as described in Section 2 (Fig. 8). Upon delivery into this simulated bile duct, the sensor was completely covered in blood and other intestinal fluids (as confirmed upon removal of the stent at the close of the test).

The coils were stabilized over the animal subject on over-hanging metal operating-room tray tables. The pig was then lowered (on the moveable surgical table) away from the coils, such that the sensor was approximately 8 in. away from the face of the coils, and a baseline measurement was taken. The pig was then moved back up to the coils. Figure 9 shows the basic arrangement of the coils and animal during this procedure. The process described here resulted in a repeatable baseline, such that the sensor response could be measured.

Figure 10(a) shows the measured sensor amplitude response, acquired when the sensor was approximately 5 cm away from the face of the coils, inside the pig. The signal-to-noise ratio is between 2 and 4. Figure 10(b) shows the measured sensor amplitude response, acquired when the sensor was approximately 2 cm away from the face of the coils, inside the pig. The sensor signal and signal-to-noise

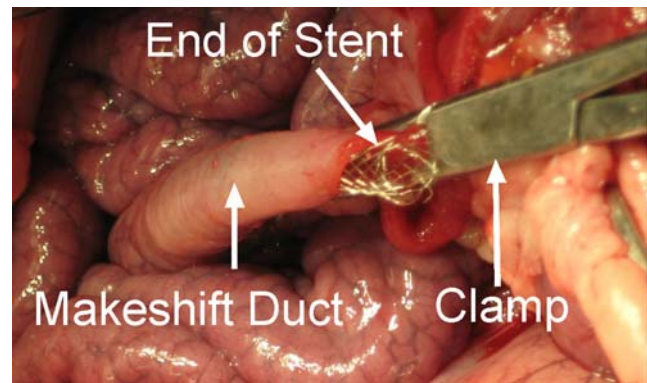


Fig. 8 A simulated bile duct of approximately 6 mm in diameter is formed using a portion of the small intestine and a clamp. The modified stent is then deployed in the duct, with the proximal portion protruding as shown here

ratio are ~18× larger than those measured from 5 cm, due to the proximity of the sensor. However, measured anti-resonant and resonant frequencies are identical.

3.3 *Ex vivo* experiment—evaluation of harvested bile

To evaluate the response of the sensor in actual, end-use biological fluids, approximately 20 mL of bile was harvested from the liver of the animal and used in a bench-top setting. The 1 mm wide × 25 mm long × 25 μm thick sensor that had been previously characterized (Section 3.1) was then used for two sets of experiments with the harvested bile. The first set of experiments was intended to determine if the viscosity of the harvested bile could be directly measured by the sensor, whereas the second set was intended to determine the influence of bile on the response of a sensor that is imbedded in sludge simulant.

For the first set of experiments, the sensor was directly immersed in the bile (at room temperature) and the

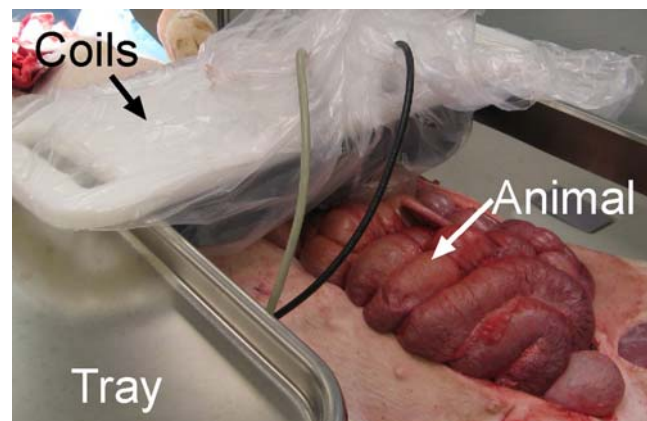


Fig. 9 The coils are stabilized over the animal using overhanging metal trays. The animal is lowered away from the coils so a baseline can be measured. The animal is then raised back into position for interrogation of the sensor

¹ All surgical procedures in this experiment were performed by R. Kwon.

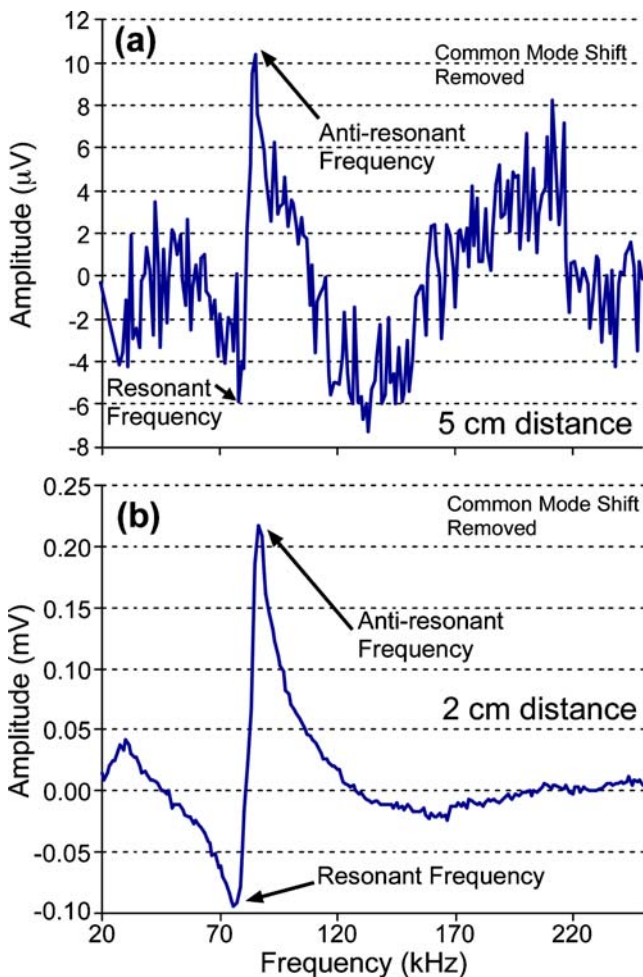


Fig. 10 (a) Measured amplitude response for the implanted sensor at a distance of 5 cm from the face of the coils. (b) Measured amplitude response for the implanted sensor at a distance of 2 cm from the face of the coils. The displayed signals have the baselines subtracted

response was measured. The measured $\Delta f/f_0$ was used to back-calculate the square root of the density-viscosity product using the calibration curve. Assuming the density of bile is near that of water, the viscosity of bile is estimated to be between 2.75 and 3.68 \times that of water (Fig. 7), which is in good agreement with literature (Jungst et al. 2001).

For the second set of experiments, the same 1 mm \times 25 mm \times 25 μ m ribbon-shaped sensor was placed in a 6 mm (inner diameter) plastic tube, which was then filled with a 3:1 by-weight ratio mixture of 500 cS silicone fluid (Dow Corning) and polyvinyl butyral powder to act as a sludge simulant. Then, a rough 3–4 mm diameter open flow channel was made in the sludge simulant. The response of the sensor while placed in the tube and loaded by sludge simulant was first measured in air and then while immersed in the harvested bile. The response of the sensor loaded by sludge simulant was different from the response of the unloaded sensor, including a decrease in both quality factor and characteristic frequency. The simulated sludge loading also

produced a much larger magnitude of shift in the sensor response than did the immersion of the unloaded sensor in bile. However, no statistically significant difference was seen between the response of the sludge-loaded sensor in air and the response of the sludge-loaded sensor immersed in bile, indicating that the sensor responds preferentially to the loading provided by the sludge simulant. This comparison included measurements of signal amplitude, phase-dip center frequency, phase-dip half-power bandwidth, and resonant frequency. It is hypothesized that the presence of the highly viscous sludge simulant shields the sensor from the viscous effects of the fluid in the flow channel. This effect makes physical sense due to the decay of the shear waves as the vibrations pass through the viscous sludge stimulant (Darvennes and Pardue 2001). In the end-use application, this shielding effect is potentially beneficial, because the knowledge of the presence (and amount) of sludge is more desirable information than knowledge of shifts in viscosity once sludge has begun to accumulate.

4 Future work and conclusions

One of the challenges in the practical use of the implanted sensor is expected to be the baseline measurement due to the presence of parasitic coupling between the coils and nearby conductors (such as bodily tissues, implants, and parts of surgical equipment). This coupling is governed by the permeability, permittivity, and conductivity of the objects, and generally exhibits a frequency dependent value. The conductivity of the materials results in eddy currents due to the time-varying magnetic field supplied by the coils. The fact that the permeability, conductivity and/or permittivity of the conductor materials changes with frequency means the eddy currents will also change with frequency, shifting the mutual coupling (i.e. shifting the baseline) when these conductors are brought near the coils. An ideal arrangement would permit the baseline measurement to be taken with the subject in place, but with the sensor turned “off”, thus accounting for all of the parasitic couplings. In the future, it might be possible to turn the sensor “on” and “off” through the use of an externally applied DC magnetic field. Future efforts may also include measurement of the implanted sensor response as the stent is perfused with relevant materials like bile, blood, or sludge.

The implantation of a commercially-available metal biliary stent enhanced with a magnetoelastic sensor and conformal magnetic layer into a pig carcass allowed for the confirmation of a measurable sensor response in a situation that mirrors the envisioned end-usage. A response from the implanted sensor was measurable with at least 5 cm of wireless range, while the sensor was covered with digestive fluids. Bile was harvested from the animal and its effect on

the sensor response was compared with effects on the sensor response from fluids of known properties. The results of this comparison, showing an estimated bile viscosity of 2.7–3.7 cP, verified the suitability of the fluids for use as bile substitutes in future tests. Overall, the results of the experiments described in this paper demonstrate the fundamental usability of the sensor in *in situ* and *ex vivo* contexts.

Acknowledgements Metglas Inc., Hoosier Magnetics, and Dow Corning provided samples for this project. This work was supported in part by a National Science Foundation (NSF) Graduate Research Fellowship to S. Green, the NSF ERC for Wireless Integrated Microsystems (WIMS), and the University of Michigan.

References

- ASM Handbook, vol. 16, (ASM International, 1989)
- A. Colas, J. Curtis, in *Biomaterials Science: An Introduction to Materials in Medicine*, ed. by B. Ratner, A. Hoffman, F. Schoen, J. Lemons, 2nd edn. (Elsevier Academic, London, 2004), p. 80
- C. Darvennes, S. Pardue, Boundary effect of a viscous fluid on a longitudinally vibrating bar: theory and application. *J. Acoust. Soc. Am.* **110**(1), 216–224 (2001)
- G. Donelli, E. Guaglianone, R. Di Rosa, F. Fiocca, A. Basoli, Plastic biliary stent occlusion: factors involved and possible preventive approaches. *Clin. Med. Res.* **5**(1), 53–60 (2007)
- G. Engdahl (ed.), *Handbook of Giant Magnetostrictive Materials* (Academic, London, 2000), pp. 1–19
- S. Green, Y.B. Gianchandani, Wireless magnetoelastic monitoring of biliary stents. *J. Microelectromech. Syst.* **18**(1), 64–78 (2009)
- S. Green, Y.B. Gianchandani, Tailored magnetoelastic sensor geometry for advanced functionality in wireless biliary stent monitoring systems. *J. Micromech. Microeng.* (2010), in review
- D. Jungst, A. Niemeyer, I. Muller, B. Zundt, G. Meyer, M. Wilhelmi, R. del Pozo, Mucin and phospholipids determine the viscosity of gallbladder bile in patients with gallstones. *World J. Gastroenterol.* **7**(2), 203–207 (2001)
- R. Kozarek, Metallic biliary stents for malignant obstructive jaundice: a review. *World J. Gastroenterol.* **6**(5), 643–646 (2000)
- L. Lagorce, M. Allen, Magnetic and mechanical properties of micromachined strontium ferrite/polyimide composites. *J. Microelectromech. Syst.* **6**(4), 307–312 (1997)
- D. Nelson, Expandable metal stents: physical properties and tissue responses. *Tech. Gastrointest. Endosc.* **3**(2), 70–74 (2001)
- J. Sung, Bacterial biofilm and clogging of biliary stents. *J. Ind. Microbiol.* **15**, 152–155 (1995)